

Description of Atmospheric Conditions at the Pierre Auger Observatory

Using Meteorological Measurements and Models

Bianca Keilhauer^{1a} and Martin Will^{1b} for the Pierre Auger Collaboration^{2c}

¹ Karlsruhe Institut für Technologie, Institut für Kernphysik, Karlsruhe, Germany

² Observatorio Pierre Auger, Av. San Martín Norte 304, 5613 Malargüe, Argentina

Received: August 14, 2019/ Accepted: date

Abstract Atmospheric conditions at the site of a cosmic ray observatory must be known well for reconstructing observed extensive air showers, especially when measured using the fluorescence technique. For the Pierre Auger Observatory, a sophisticated network of atmospheric monitoring devices has been conceived. Part of this monitoring was a weather balloon program to measure atmospheric state variables above the Observatory. To use the data in reconstructions of air showers, monthly models have been constructed. Scheduled balloon launches were abandoned and replaced with launches triggered by high-energetic air showers as part of a rapid monitoring system. Currently, the balloon launch program is halted and atmospheric data from numerical weather prediction models are used. A description of the balloon measurements, the monthly models as well as the data from the numerical weather prediction are presented.

PACS. 95.85.Ry Cosmic rays – 95.55.Vj Cosmic ray detectors – 92.60.-e Properties and dynamics of the atmosphere

1 Introduction

At the Pierre Auger Observatory, extensive air showers induced by cosmic rays with energies above 10^{17} eV are measured. With increasing energy of the primary particle, the flux of cosmic rays is strongly decreasing and it is expected that a transition from cosmic rays with galactic origin to those with extragalactic origin is occurring in the observed energy range of the Pierre Auger Observatory. Besides the energy of the cosmic rays, which is needed to evaluate the spectral slope of the cosmic ray flux, another information of utmost importance is their mass composition. For the detection of extensive air showers with high statistics, a surface detector array consisting of more than 1 600 water Cherenkov tanks is installed at the Pampa Amarilla close to Malargüe, Argentina. The second component of the Observatory are 27 fluorescence telescopes at four sites observing faint nitrogen fluorescence in the atmosphere above the ground array. The fluorescence emission is induced by the giant cascade of secondary particles developing after the primary cosmic ray interacts with nuclei in the upper parts of the atmosphere. This dim light can only be detected during nights with low atmospheric opacity and little light background from the moon or other sources.

The fluorescence technique is very susceptible to changes in atmospheric state variables and optical properties of the air. Both depend on air temperature, pressure and on water vapor pressure. For this reason, the Pierre Auger Observatory employs a sophisticated atmospheric monitoring program [1] to measure atmospheric properties. This includes infrared cloud cameras and lidar stations at every FD site [2] to scan for clouds, a weather balloon program [3] to measure profiles of atmospheric state variables and five weather stations distributed over the array of the Auger Observatory to monitor surface values. The lidar stations and two central laser facilities are used to measure the aerosol optical depth [4]. All this information is adequately processed to be included in the reconstruction procedure for measured extensive air showers. Critical aspects are the spatial and temporal resolution of the locally observed atmospheric conditions. In case of profiles of atmospheric state variables, monthly models were compiled using ra-

^a bianca.keilhauer@kit.edu

^b martin.will@kit.edu

^c http://www.auger.org/archive/authors_2012_06.html

diosonde data [3]. More recently, the applicability of data from the Global Data Assimilation System (GDAS) for the Pierre Auger Observatory has been investigated [5].

The paper is structured as follows: In Sec. 2, we will give a short introduction to expected effects of atmospheric properties on the development and detection of extensive air showers. The locally observed data of state variables by weather balloons and their application in the air shower reconstruction are described in Sec. 3. In Sec. 4, GDAS data are described and compared to local measurements at the Auger Observatory and the development of monthly models from these data is detailed. A brief discussion of uncertainties within the air shower reconstruction caused by variations of atmospheric conditions is given in Sec. 5.

2 Impact of Atmospheric State Variables on Air Shower Measurements

Two important aspects of air shower reconstruction are the determination of the energy of the primary particle of each shower and the estimate of the mass composition for a large set of observed events. The first quantity is obtained at the Pierre Auger Observatory by an almost calorimetric measurement of the energy deposited in the atmosphere during the air shower development [6]. The induced fluorescence light is proportional to the energy deposit at each state of shower development [7]. The integral detection of the light trace by fluorescence telescopes enables a very precise determination of the energy of the cosmic ray particle. The second quantity, the mass composition of air showers, is derived by investigating the position of the shower maximum X_{\max} , the altitude given in units of g cm^{-2} where the number of secondary particles is highest [8]. For the general case of vertical incidence and equal energy of the primary cosmic ray particle, nuclei of light elements initiate deeply penetrating air showers and more shallow showers are formed by interactions of heavier elements. X_{\max} is fluctuating considerably from shower to shower, so large statistics is needed to draw conclusions about mass composition. Larger fluctuations of X_{\max} are observed for lighter elements than for elements with a high number of nuclei. With fluorescence telescopes, the atmospheric depth of shower maximum can be measured directly.

Atmospheric state variables, mainly the density of air ρ , alter the development of extensive air showers in the atmosphere as it is governed by the interactions and decays of the secondary particles. These processes are determined by the atmospheric depth X , which is the path integral of ρ from the top of the atmosphere to a given altitude. Since the fluorescence telescopes observe the light trace with respect to geometrical altitude h , the conversion between h and X depends on atmospheric conditions.

Most sensitive to short-term variations of state variables is the fluorescence yield of nitrogen in air [9–12]. The main emission bands for nitrogen molecules are in the range between about 280 and 420 nm. The energy deposit of the air shower in the atmosphere causes an excitation of mainly the second positive system of N_2 and the first negative system of N_2^+ . The spontaneous de-excitation, yielding the fluorescence light emission, is counteracted by collisional de-excitation of nitrogen molecules by other nitrogen or oxygen molecules and by water vapor. These quenching processes are dependent on atmospheric conditions. The rate of collisions between the molecules can be described by kinetic gas theory, including temperature and pressure dependence. In addition, the collisional cross sections between nitrogen and air molecules in general were measured to be explicitly temperature-dependent [13,14]. The content of water vapor in air adds another quenching source.

All these aspects require a sophisticated consideration of actual atmospheric conditions in the process of air shower reconstruction. Thus, the Pierre Auger Observatory is operating a program for measuring profiles of atmospheric state variables with meteorological radio soundings supplemented by a set of ground-based weather stations.

3 The Weather Balloon Program

In the process of air shower reconstruction, the observed fluorescence light at the telescopes is interpreted as energy deposited by the air shower in the atmosphere along the shower trajectory. This requires intermediate steps of correcting the observed light by atmospheric attenuation (absorption and scattering out of the field of view) and of determining the effective fluorescence yield taking into account all quenching processes. The atmospheric properties needed for fluorescence description are described in Sec. 2. In the case of ground-based fluorescence telescopes, like the detectors used at the Auger Observatory, light absorptions by atmospheric trace gases is of minor importance. More relevant are aerosol and molecular scattering. Aerosol conditions above the Observatory are measured every hour during data taking of the telescopes [4]. The molecular scattering, i. e. Rayleigh scattering, depending on temperature, pressure and humidity, is calculated during reconstruction by applying atmospheric profiles of these quantities.

3.1 Radiosoundings

The most direct way to obtain altitude-dependent profiles of state variables is given by measurements with meteorological radiosondes launched on weather balloons. At the Pierre Auger Observatory, intermittent launches were

performed between August 2002 and December 2010. During the first years, campaigns of about 3 weeks with an average of 9 launches per campaign were done roughly 3 times per year. Starting in July 2005, the rate of launches became more regularly to about one launch every five days. In March 2009, the radio soundings were implemented into the rapid atmospheric monitoring program of the Auger Observatory [3], triggering a launch of a weather balloon shortly after the detection of particularly interesting air showers like very high-energetic events, see Sec. 3.3. In total, 331 successfully measured profiles are gathered until end of 2010.

With the used radiosondes [16], air temperature T and relative humidity u are measured directly via dedicated sensors. Until October 2008, a type of radiosonde was used with active measurement of the pressure p . With the more recent type of sonde, the pressure is calculated iteratively from ground pressure, the measured temperature profile and altitude from GPS information. The wind speed and direction is obtained from the GPS position as well. All derived variables like water vapor pressure and air density are calculated afterwards. In Fig. 1, one example measurement of the atmospheric conditions per season is displayed. Because of the exponential decrease of p , this variable is plotted as difference to the US Standard Atmosphere 1976 (USStdA) [15]. Significant differences to the USStdA are found between about 5 and 12 km a.s.l. where the most dynamic development of extensive air showers is taking place. Air humidity is relevant only in the lowest 6 km a.s.l., influencing mainly the air fluorescence yield (see Sec. 2). The main wind direction is west at the site of the Auger Observatory, only few balloons were driven by east wind. As indicated by the altitude color code¹ in the bottom panel of Fig. 1, most of the weather balloons were still above the array of the Observatory until about 10 km a.s.l., the conditions were indeed measured at the place of interest.

3.2 Monthly Models

Radiosonde launches are the most accurate way to determine the current profiles of atmospheric state variables for air shower reconstruction. Meteorological institutions performing synoptic measurements around the world launch at least two balloons per day, while at the Pierre Auger Observatory, only one balloon every few days was launched. Even though the atmospheric conditions above the Pampa Amarilla vary only moderately, it is not possible to simply interpolate between two launches for the application in air shower reconstruction. To cover all periods and in particular the intermediate time periods, monthly models have been constructed for the site of the Observatory. These models have been compiled two times from locally measured weather data, once in 2005 and an updated set was produced in 2009. The models from 2005 are mostly based on radiosonde measurements from Córdoba and Santa Rosa, Argentina, both more than 500 km away from Malargüe. They are adjusted in the lower part of the atmosphere by local radiosonde launches performed above the Pierre Auger Observatory.

Until December 2008, 277 launches were performed on site, so models based solely on local measurements could be produced. Unlike the previous version, this new set also includes air humidity. All data measured during day and night are used, but some criteria are applied to the dataset to avoid biasing the monthly models. If there are more than one launch performed within one day or within one night, only one data set is selected for the models. Therefore, only one launch per nine hours is considered. This leaves data from 261 launches. For the monthly vapor pressure models, 32 more launches during overcast conditions are excluded.

For each launch, measured temperature, pressure and relative humidity profiles are available. Vapor pressure and density are then calculated using the Magnus formula and the ideal gas law. Profiles of the atmospheric depth are calculated by integrating the density profile from the height at balloon burst h_b down to the ground. The initial atmospheric depth at burst height is estimated by the pressure and the gravitational acceleration, $X(h_b) = p(h_b)/g(\Phi, h_b)$, with Φ being the geographical latitude. Typical burst heights are between 20 and 25 km corresponding to atmospheric depths between 20 to 40 g cm⁻². All profiles of each month are then averaged giving profiles starting at 1 600 m a.s.l. Using data from five weather stations across the Observatory, the averages are extrapolated down to 1 200 m a.s.l. The monthly profiles for temperature T and water vapor pressure e are displayed in Fig. 2, along with the differences of pressure p and atmospheric depth X to the profiles of the USStdA.

For an appropriate use in air shower simulations, e. g. using CORSIKA [17], every monthly atmospheric depth average is fitted with an exponential function for four different layers i ,

$$X(h) = a_i + b_i e^{-h/c_i}. \quad (1)$$

The four sets of parameters a_i , b_i , c_i and the heights of the boundaries between the layers are fit taking into account given boundary and continuity conditions between the layers. The local models reach up to 30 km, but for air shower simulations, data are required until the top of the atmosphere. This is achieved by applying adjusted density data from the USStdA above the local profiles up to 100 km. Above, the atmospheric depth is described by a linear decrease to Zero which is reached at 112.8 km a.s.l. This fifth layer is adopted from the standard parameterization of the USStdA which is available in CORSIKA.

¹ For interpretation of the colors in this figure, the reader is referred to the web version of this article.

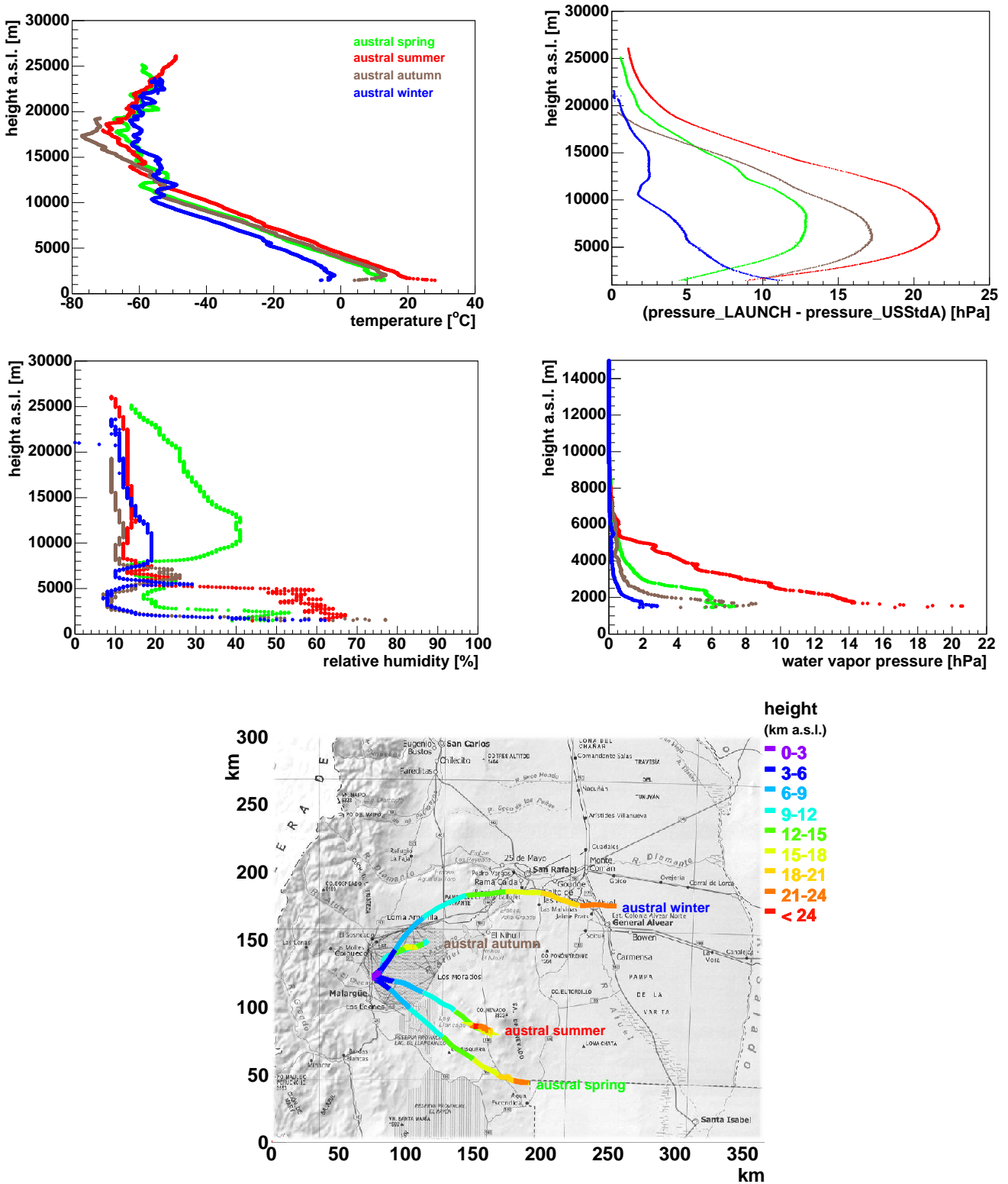


Figure 1. One characteristic atmosphere per season obtained by meteorological radiosondes above the array of the Pierre Auger Observatory. The profiles for spring were measured at Oct., 3rd, 2007, 9:17 UTC (start time of weather balloon), for summer at Feb., 19th, 2008, 00:29 UTC, for autumn at Apr., 28th, 2007, 9:26 UTC, and for winter at Aug., 10th, 2007, 9:26 UTC. Top left: temperature, Top right: difference of measured pressure profile to that of the US Standard Atmosphere 1976 (USStdA) [15], Bottom left: relative humidity, Bottom right: water vapor pressure. Bottom: Flight path of weather balloons¹.

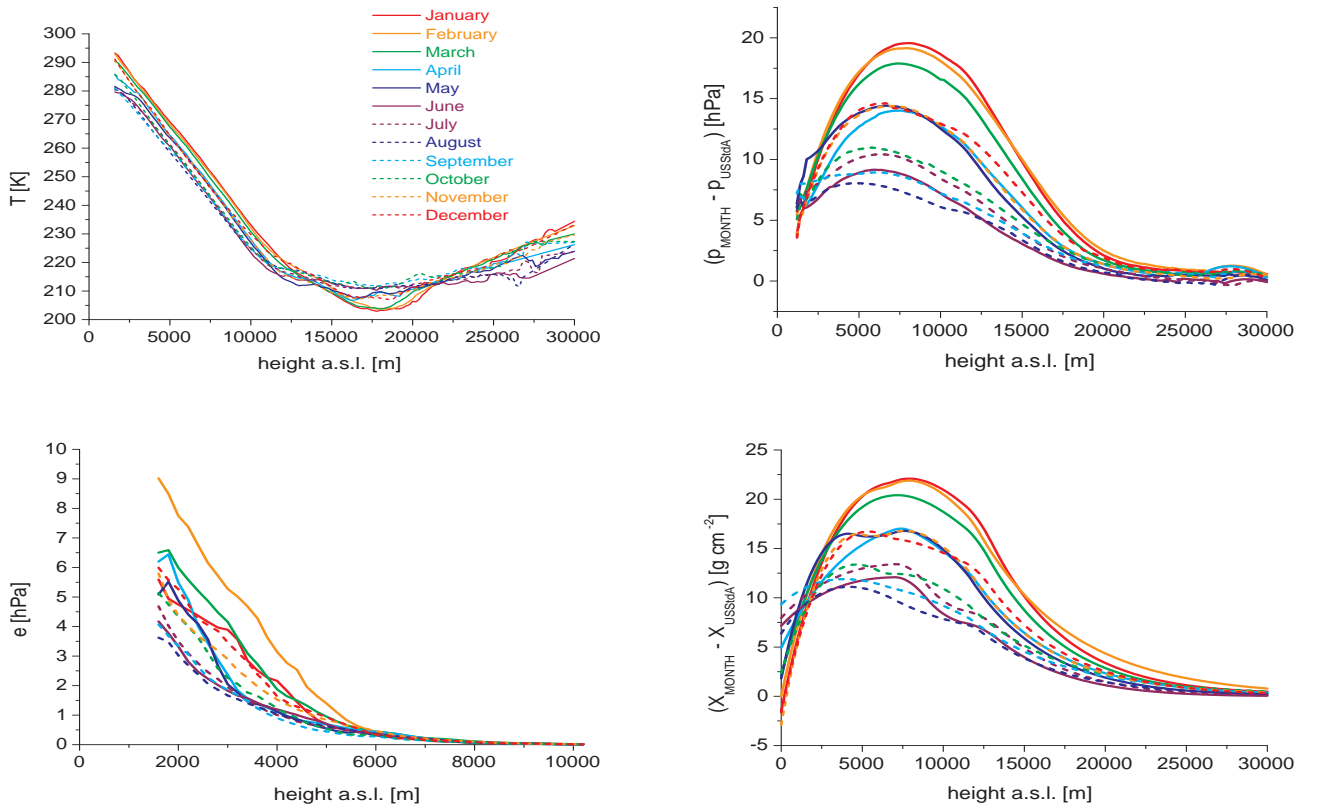


Figure 2. The Malargüe Monthly Models for temperature, pressure, water vapor pressure and atmospheric depth derived from local measurements until end of 2008. For pressure and atmospheric depth, the difference to the USStdA is shown.

3.3 The Balloon-the-Shower program

The rapid atmospheric monitoring program is conceived to provide almost real-time atmospheric data for air shower events that are of special interest to the analyses of the Pierre Auger Observatory [3]. This includes events with very high energies that are used for the energy calibration of the SD array [18] as well as anisotropy and composition studies [19, 20]. Also, showers with distorted profiles are of interest, since they might arise from exotic particles or unusual hadronic interactions [21]. To be able to trigger a dedicated atmospheric measurement, air shower data are put to an online reconstruction within a few minutes after they are gathered in the central campus of the Observatory.

The balloon program became part of this program in March 2009 to reduce the time after an high-energetic air shower from up to several days down to less than three hours. Relevant air shower parameters, like reconstructed energy, shower profile, detector information and uncertainty estimates, from the online reconstruction are sent to a computer running an analysis script that checks for new showers every 15 minutes for profiles that meet certain quality criteria. In order to reduce the number of possible air showers triggering the *BtS* (Balloon-the-Shower) program, an energy threshold of $10^{19.3}$ eV (about 20 EeV) was implemented.

Once an interesting shower is found, a local technician is informed via a short text message. He then drives to the Balloon Launching Station (BLS, c.f. Fig. 3) close to the south-western boundary of the surface detector array to launch a probe. Radiosondes are launched only within 3 hours after the time of an air shower event. During the run of *BtS* between March 2009 and December 2010, 100 interesting showers were identified, followed by sending a text message, and yielding 52 successfully launched balloons. During some launches, further triggers were registered, so that a total number of 62 air shower events are covered by actual radio soundings. The remaining triggers were lost due to diverse technical failures.

An analysis of reconstructed shower parameters with profiles measured within the *BtS* program instead of monthly models shows a clear improvement of the accuracy of the reconstruction and no systematic effect due to shower geometry or time of year are found, see Sec. 5. The *BtS* data played an important part in validating new atmospheric model data for the air shower reconstruction at the Pierre Auger Observatory. The on-site measurements served as

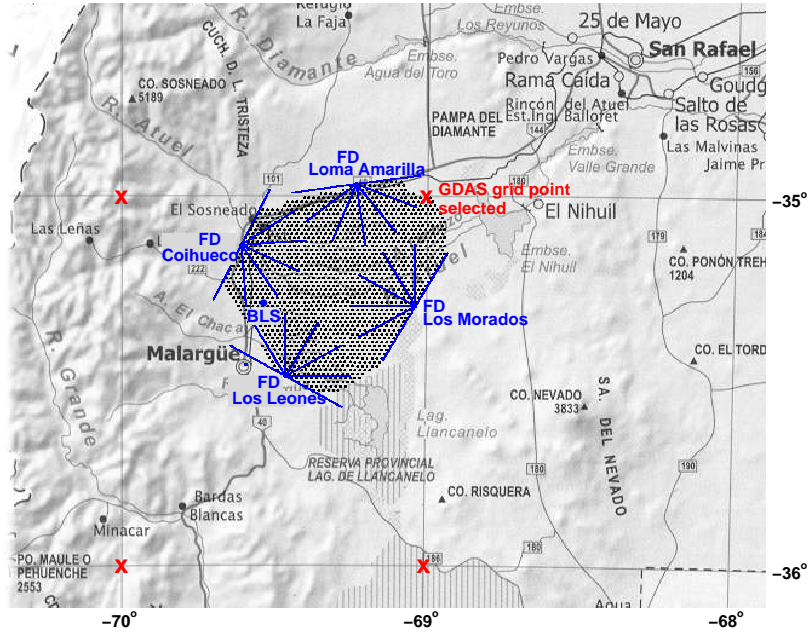


Figure 3. Map of the region around the Pierre Auger Observatory with geographical latitudes and longitudes marked at the boundary of the figure. The positions of the surface and fluorescence detectors are superimposed. The GDAS grid points closest to the Observatory are marked as red crosses. The coordinates of Malargüe are -35.48° (south) and -69.58° (west).

a reference for investigating the applicability of data from the Global Data Assimilation System (GDAS) for the Observatory, see next Section.

4 Data From Numerical Weather Prediction

Nowadays, numerical weather prediction is based on the process of *data assimilation*. Using complex mathematical models, the atmospheric conditions can be predicted at all positions worldwide. To consolidate these models, the predictions are supplemented with measured data from weather stations, weather balloon launches, measurements from aircraft and ships, as well as satellite data.

4.1 The Global Data Assimilation System

The Global Data Assimilation System (GDAS) is provided by the American National Oceanic and Atmospheric Administration (NOAA). The data are available in a resolution of three hours and a 1° latitude-longitude grid for the entire globe without charge via NOAA’s Real-time Environmental Applications and Display sYstem (READY) [22]. In Fig. 3, the available grid points close to the Auger array are shown. Superimposed are the positions of the regular SD grid and the location and field of views of the four FD sites. The two grid points to the West of the Observatory are already in the Andes mountains and therefore not suited. The point to the North-East was chosen as it is the closest to the array. The differences between this point and the grid point to the South-East are on average less than 1°C in temperature and less than 0.3 hPa in water vapor pressure at all altitudes, making an extrapolation unnecessary.

GDAS data is provided on 23 pressure surfaces ranging from 1000 hPa (sea level) to 20 hPa (about 26 km a.s.l.). Additionally, surface values are included. For the site of the Auger Observatory, the lowest 5 pressure levels are below the surface height. This is a remnant of the mathematical nature of the numerical weather prediction model and the data of these levels are discarded. Useful data for the Auger site are available starting in June 2005.

To check the applicability of the GDAS data at the Auger site, they were compared with the local radiosonde data and weather station data on the ground. In Fig. 4, for several altitudes the differences in temperature, pressure, water vapor pressure and atmospheric depth between measured radiosonde data and the corresponding data from the GDAS model (black dots) and the Malargüe monthly models (red open squares) are shown for measurements in 2009

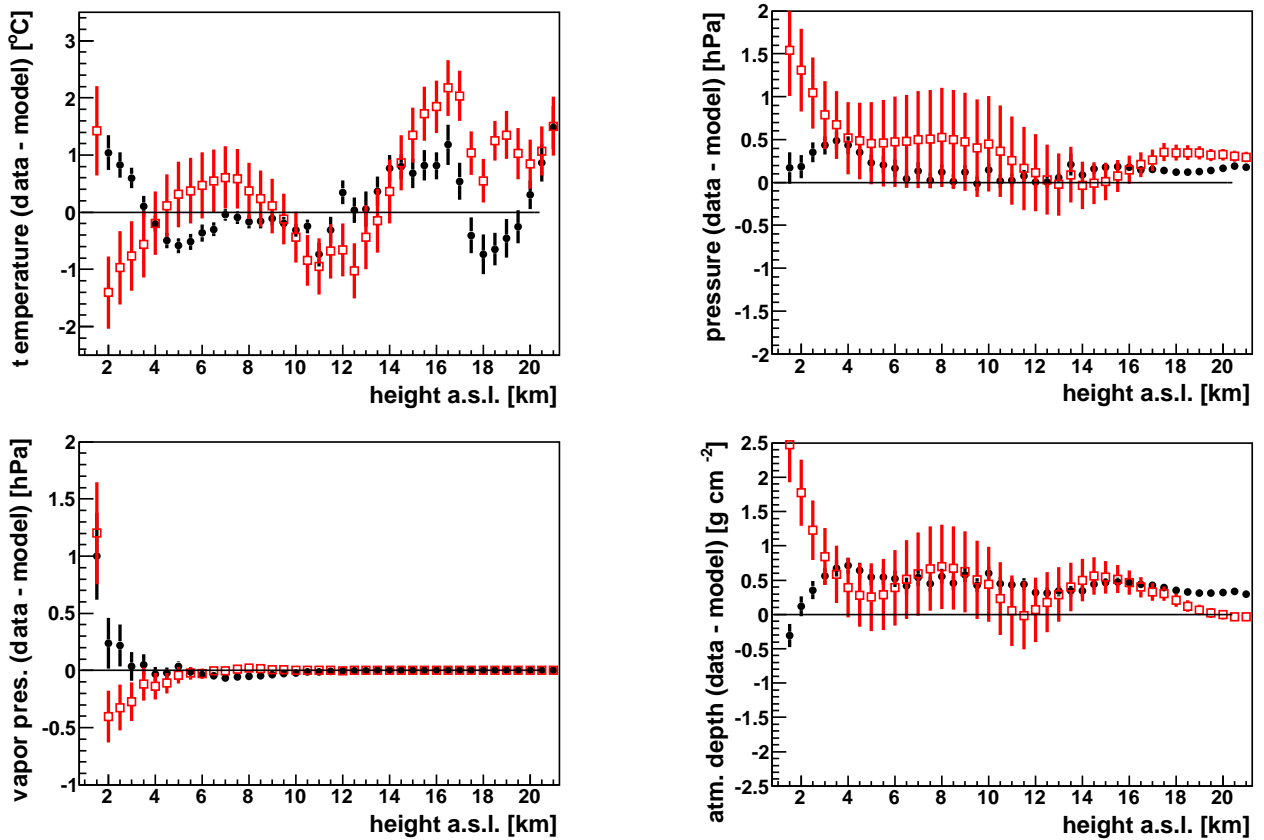


Figure 4. Average difference of measured radiosonde data and GDAS models (black dots) and monthly mean profiles (red squares) versus height for all radiosondes performed in 2009 and 2010. Error bars denote the RMS spread of the difference.

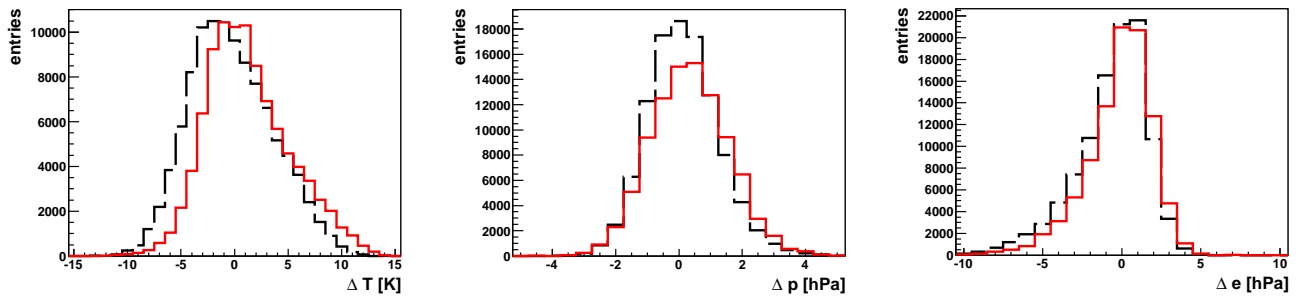


Figure 5. Difference of measured weather station data and GDAS models for all data from 2009. The differences GDAS model minus measured data in temperature T , pressure p , and water vapor pressure e are shown for the weather station at the CLF (solid red line) and the station at FD Loma Amarilla (dashed black line).

and 2010. This time period was chosen since the monthly models were compiled from data until the end of 2008, so the balloon data from 2009 and 2010 represent an independent data sample to the monthly models. The error bars denote the RMS of the differences at each height. Closer to the ground, slightly larger differences are found in all quantities. In all four quantities, both models describe the local conditions well. However, it is clear that the GDAS model overall shows slightly smaller differences than the monthly models and, more importantly, has much smaller deviations between individual profiles as indicated by the much smaller error bars. It should be mentioned that the agreement between local radio soundings and the monthly models is similarly well as the GDAS model comparison with local measurements for the years 2005 to 2008 [5], but still GDAS has a smaller spread.

The surface values of the GDAS data are investigated by comparisons with data from the weather stations. In Fig. 5, the differences of measured weather station data and GDAS data are shown for two weather stations (CLF and

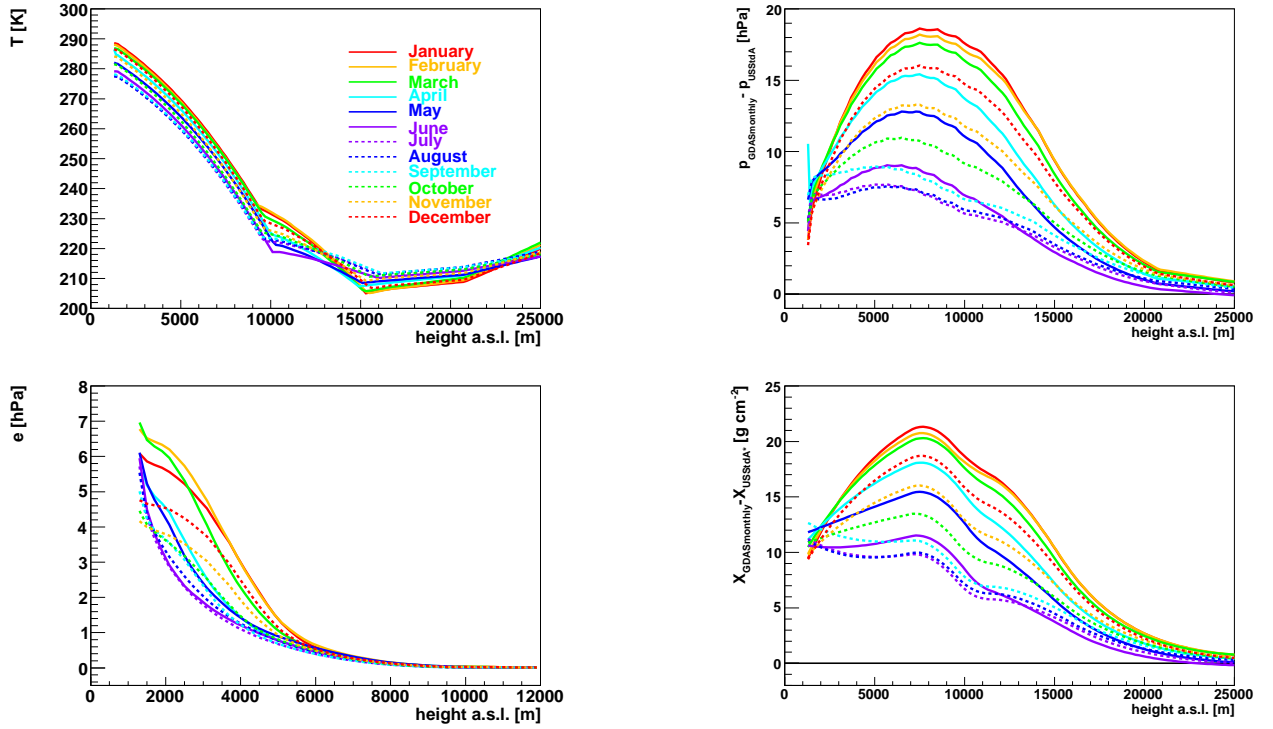


Figure 6. Monthly averages after fit and self-consistency procedures for temperature T , pressure p , water vapor pressure e and atmospheric depth X . Pressure and atmospheric depth are shown in difference to the US Standard Atmosphere.

Loma Amarilla) at the time of the GDAS data set. The GDAS data are interpolated at the height of the respective weather station and agree well with the weather station data. The mean deviation of the distributions is comparable to the difference seen between individual weather stations across the array.

In summary, the GDAS data describe the conditions at the Pierre Auger Observatory very well as shown by comparisons with locally measured data. With its superior temporal resolution, they are an excellent source for profiles of atmospheric state variables. Furthermore, the GDAS data sets contain a lot more information that might be explored in the future.

4.2 Monthly Models from GDAS Data

The 3-hourly GDAS data are very well suited for data reconstruction at the Pierre Auger Observatory, as shown in the previous section. For air shower simulations, e. g. with CORSIKA, a parameterized atmospheric depth is needed. This is a complex procedure and cannot be repeated every three hours for GDAS data, resulting in an excessive number of possible atmospheric conditions to choose from during simulations. Therefore, GDAS data are not applicable for simulation. Monthly models are a good compromise between mapping seasonal atmospheric variations on air shower development and exploiting the good agreement of GDAS data at the Auger site. Averaging the GDAS data in monthly bins for the time period of June 2005 until May 2011 shows clear seasonal trends at all altitudes for temperature, pressure, water vapor pressure, air density and atmospheric depth.

After creating monthly averages of all relevant atmospheric state variables, the atmospheric depth is fit with an exponential function, see Eq. (1), and for all 12 months, the atmospheric depths profiles are parameterized as described in Sec. 3.2. The parameterized atmospheric depth functions describe the averaged depth profiles very well, only showing small differences of less than 0.5 g cm^{-2} at all altitudes. These residuals are much smaller than those for the monthly models because of the rather small number of local measurements used to develop the models as described in Sec. 3.2.

For using the monthly GDAS models in air shower reconstructions as a fallback if the 3-hourly GDAS data are not available, the models for the temperature, pressure, humidity and air density have to be provided, along with the depth parameterizations. However, after the fit procedure, the model of the atmospheric depth is not necessarily consistent with the averages of the other variables. Therefore, new air density profiles are computed from the derivatives of the depth parameterizations. Using the averaged pressure profile, a new temperature profile is calculated using the ideal gas law and new profiles of the water vapor pressure and relative humidity can be compiled. The new profiles are checked

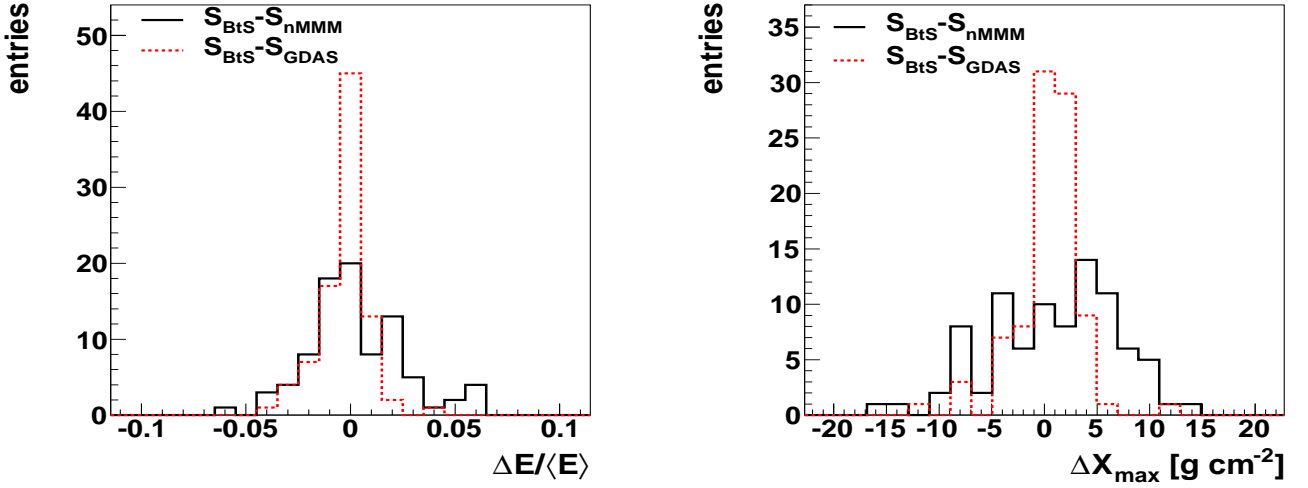


Figure 7. Energy difference (left) and difference of position of shower maximum (right) between events recorded within the *BtS* program. The air showers are reconstructed with three different atmospheric descriptions, details see text.

against the averaged profiles and the differences are found to be of the order of the statistical uncertainties of the averaged models. In Fig. 6, the final models for temperature, pressure, water vapor pressure and the parameterizations of the atmospheric depth are shown.

5 Reconstruction of Extensive Air Showers

As a final check of the applicability of the meteorological model data for the measurements of the Pierre Auger Observatory, air shower data are reconstructed. In this analysis, the two most important air shower parameters, primary energy E and atmospheric depth of shower maximum X_{\max} , are investigated. The same set of air shower events is reconstructed in the same way with three different atmospheric descriptions. To be able to use real-time atmospheric profiles, all air showers of the *BtS* program are used. These 62 events are reconstructed one time with the atmospheric profiles of the dedicated radio soundings, labelled S_{BtS} . The second reconstruction set is processed using the monthly models from local measurements (Sec. 3.2), S_{nMMM} , and the third set is produced applying the GDAS data with the 3-hour resolution, S_{GDAS} . In Fig. 7, the differences for E and X_{\max} are shown between the different sets of reconstructions. For $S_{\text{BtS}} - S_{\text{nMMM}}$, the mean difference in the reconstructed energy is 0.5% and the width of the distribution is 2.3%, in X_{\max} the difference is 0.3 g cm^{-2} with an RMS of 6.6 g cm^{-2} . For $S_{\text{BtS}} - S_{\text{GDAS}}$, the mean difference in the reconstructed energy is -0.2% with an RMS of 1.2%, and 0.5 g cm^{-2} with a width of 3.3 g cm^{-2} in X_{\max} . While the mean differences are centered about zero, the spread of the distribution of the $S_{\text{BtS}} - S_{\text{nMMM}}$ comparison is not negligible for the uncertainties of air shower reconstructions.

Applying the atmospheric data from GDAS presented here in an air shower simulation study, the advantage of the data is demonstrated. The reconstruction uncertainties related to the description of the molecular atmosphere decrease by as much as 50% using the GDAS data instead of the monthly models [5]. This result was obtained by simulating air showers with arbitrary geometries using atmospheric conditions measured by radiosondes. After reconstructing these data with the correct measured data, the GDAS data and the monthly models, the uncertainties can be evaluated by comparing the reconstructions using the models and the correct atmospheric conditions.

6 Summary

Atmospheric monitoring and the better understanding of fluorescence emission processes in the atmosphere are very important tasks for ground-based cosmic ray observatories, as they contribute a large part to the total systematic uncertainties of reconstructed parameters.

At the Pierre Auger Observatory, atmospheric state variables at the ground are measured continuously by several weather stations and an extensive weather balloon program was operated to measure the height-dependent profiles of these parameters. To use this information in the reconstruction of air showers, monthly models have been constructed from monthly averages of these balloon data. To improve the reconstruction quality of showers of special interest, a

rapid monitoring program was implemented to launch balloons after high-energetic events that are identified by an online reconstruction.

Following the balloon program, GDAS data are now processed for using in the analyses procedures of the Pierre Auger Observatory. With their superior temporal resolution and good availability, they are suited perfectly for the reconstruction of air showers and help to significantly reduce the systematic uncertainties associated with the choice of the model to describe the molecular atmosphere. From these data, monthly models were constructed to help to incorporate our best knowledge of the atmosphere above the Pierre Auger Observatory also in the simulations of cosmic ray air showers.

Acknowledgments

We would like to thank the organizers of the workshop *Interdisciplinary Science @ the Auger Observatory: from Cosmic Rays to the Environment* in Cambridge, UK, 2011, and in particular A.A. Watson, for the inspiring meeting. Part of these investigations are supported by the Bundesministerium für Bildung und Forschung (BMBF) under contracts 05A08VK1 and 05A11VK1. Furthermore, these studies would not have been possible without the entire Pierre Auger Collaboration and the local staff of the Observatory.

References

1. J. Abraham et al., the Pierre Auger Collaboration, *Astropart. Phys.* **33**, 108 (2010)
2. V. Rizi, A. Tonachini, for the Pierre Auger Collaboration, in *Focus Point on Interdisciplinary Science at the Pierre Auger Observatory (2012)*, Editors: A. Bueno, L. Wiencke. EPJ Plus
3. P. Abreu et al., the Pierre Auger Collaboration, submitted to JINST (August 2012)
4. L. Wiencke, for the Pierre Auger Collaboration, in *Focus Point on Interdisciplinary Science at the Pierre Auger Observatory (2012)*, Editors: A. Bueno, L. Wiencke. EPJ Plus
5. P. Abreu et al., the Pierre Auger Collaboration, *Astropart. Phys.* **35**, 591 (2012)
6. J. Abraham et al., the Pierre Auger Collaboration, *Nucl. Instr. Meth.* **A620**, 227 (2010)
7. M. Ave et al., the AIRFLY Collaboration, *Nucl. Instr. Meth.* **A597**, 46 (2008)
8. J. Abraham et al., the Pierre Auger Collaboration, *Phys. Rev. Lett.* **104**, 091101 (2010)
9. F. Arqueros, J. Hörandel, B. Keilhauer, *Nucl. Instr. Meth.* **A597**, 1 (2008)
10. B. Keilhauer, J. Blümer, R. Engel, H. Klages, *Nucl. Instr. Meth.* **A597**, 99 (2008)
11. M. Monasor et al., *Astropart. Phys.* **34**, 467 (2011)
12. B. Keilhauer et al., in *International Symposium on Future Directions in UHECR Physics* (CERN, 2012)
13. M. Ave et al., the AIRFLY Collaboration, *Nucl. Instr. Meth.* **A597**, 50 (2008)
14. L. Pereira et al., *Eur. Phys. J.* **D56**, 325 (2010)
15. National Aeronautics and Space Administration (NASA), U.S. Standard Atmosphere 1976. NASA-TM-X-74335 (1976)
16. GRAW Radiosondes GmbH & Co. KG, Tech. rep. URL <http://www.graw.de>
17. D. Heck et al., Forschungszentrum Karlsruhe Report **6019** (1998)
18. R. Pesce, for the Pierre Auger Collaboration, in *Proc. 32nd ICRC* (Beijing, China, 2011)
19. J. Abraham et al., the Pierre Auger Collaboration, *Science* **318**, 938 (2007)
20. J. Abraham et al., the Pierre Auger Collaboration, *Phys. Rev. Lett.* **104**, 091101 (2010)
21. C. Baus et al., in *Proc. 32nd ICRC* (Beijing, China, 2011)
22. NOAA Air Resources Laboratory (ARL), Global Data Assimilation System (GDAS1) Archive Information. Tech. rep. (2004). URL <http://ready.arl.noaa.gov/gdas1.php>